34th Annual International Conference of the IEEE EMBS
San Diego, California USA, 28 August - 1 September, 2012

In vivo Manganese-enhanced MRI for Visuotopic Brain Mapping

Kevin C. Chan and Ed X. Wu*

Abstract— **This study explored the feasibility of localized manganese-enhanced MRI (MEMRI) via 3 different routes of Mn^{2+} administrations for visuotopic brain mapping of retinal, callosal, cortico-subcortical, transsynaptic and horizontal connections in normal adult rats. Upon fractionated intravitreal Mn^{2+} injection, Mn enhancements were observed in the contralateral superior colliculus (SC) and lateral geniculate nucleus (LGN) by 45-60% at 1-3 days after initial Mn^{2+} injection and in the contralateral primary visual cortex (V1) by about 10% at 2-3 days after initial Mn^{2+} injection. Direct, single-dose Mn^{2+} injection to the LGN resulted in Mn enhancement by 13-21% in V1 and 8-11% in SC of the ipsilateral hemisphere at 8 to 24 hours after Mn^{2+} administration. Intracortical, single-dose Mn^{2+} injection to the visual cortex resulted in Mn enhancement by 53-65% in ipsilateral LGN, 15-26% in ipsilateral SC, 32-34% in the splenium of corpus callosum and 17-25% in contralateral V1/V2 transition zone at 8 to 24 hours after Mn^{2+} administration. Notably, some patchy patterns were apparent near the V1/V2 border of the contralateral hemisphere. Laminar-specific horizontal cortical connections were also observed in the ipsilateral hemisphere. The current results demonstrated the sensitivity of MEMRI for assessing the neuroarchitecture of the visual brains in vivo without depth-limitation, and may possess great potentials for studying the basic neural components and connections in the visual system longitudinally during development, plasticity, pharmacological interventions and genetic modifications.**

I. INTRODUCTION

The rodents are an excellent model for understanding the mechanisms of development, plasticity and functional specialization in the visual system [1-13]. In normal adults, more than 90% of axons of retinal ganglion cells (RGCs) project contralaterally to the superior colliculus (SC) and lateral geniculate nucleus (LGN) [14, 15]. The superficial gray layer of the SC receives about 90% of its excitatory input from the retina [16] and the remainder 10% from the visual cortex [17], whereas about 30% of RGC axons project to the contralateral dorsal LGN [18], and over 90% of cells projected from the primary visual cortex (V1) lie in the ipsilateral dorsal LGN [19]. The topographic layout of the retina is represented in the SC, LGN, visual callosal fibers and each cortical visual area [20-23]. Ocular dominance plasticity is also present in rodent visual cortex [21, 24, 25]. To date, limited tools have been available for in vivo, high-resolution mapping of neuroarchitecture in the visual brains globally and longitudinally [3, 26, 27]. Mn^{2+} has been increasingly used as a T_1-weighted contrast agent for in vivo neuronal tract tracing [28-38], detection of neuroanatomy and pathophysiology [39-43] and functional brain mapping at lamina levels [33, 44-47]. In this study, we explore the capability of Mn-enhanced MRI (MEMRI) via 3 different routes of Mn^{2+} administration for in vivo assessments of retinal, callosal, transsynaptic, corticothalamic, corticocollicular and horizontal connections in normal adult rat brains.

Manuscript received March 15, 2012. This work was supported in part by the Hong Kong Research Grant Council, The University of Hong Kong CRCG grant, National Institutes of Health CORE Grant P30 EY008098, Eye and Ear Foundation of Pittsburgh, PA and Unrestricted Grant from Research to Prevent Blindness, New York, NY.

Kevin C. Chan and Ed X. Wu are with the Laboratory of Biomedical Imaging and Signal Processing and the Department of Electrical and Electronic Engineering, The University of Hong Kong, Hong Kong SAR, China (e-mail: chuenwing.chan@fulbrightmail.org, ewu@eee.hku.hk). Kevin C. Chan is also with the Departments of Ophthalmology and Bioengineering at the University of Pittsburgh; and Center for the Neural Basis of Cognition, University of Pittsburgh and Carnegie Mellon University, Pittsburgh, PA, USA.

*Ed X. Wu is the corresponding author to provide phone: (852) 2819-9713; fax: (852) 2819-9711.

II. MATERIALS AND METHODS

A. Animal Preparation

Adult Sprague-Dawley rats (N=17) were divided into 3 groups. In Group 1 (n=4), a fractionated dose of Mn^{2+} at 3μL and 50mM each was injected intravitreally into the left eye every day for a total of 3 days; In Group 2 (n=6), Mn^{2+} was injected unilaterally into the left lateral geniculate nucleus (LGN) at 30nL and 100mM; In Group 3 (n=7), Mn^{2+} was injected intracortically to the V1/V2 transition zone of the right visual cortex at 100nL and 100mM. For Group 1, MEMRI was performed before, and at 1, 2 and 3 days after initial Mn^{2+} intravitreal injection. For Groups 2 and 3, MEMRI was performed at 1 hour, 8 hours and 1 day after Mn^{2+} administration.

B. MRI Protocols

All in vivo MRI measurements were acquired utilizing a 7 T Bruker scanner using a 72 mm birdcage transmit-only RF coil and an actively decoupled receive-only quadrature surface coil. Under inhaled isoflurane anaesthesia (3% induction and 1.5% maintenance), animals were kept warm under circulating water at 37°C with continuous monitoring of the respiration rate. 2D T1-weighted (T1W) spin-echo RARE pulse sequence was acquired with repetition time/echo time (TR/TE) = 475/8.8 ms, field of view/slice thickness (FOV/th) = 32x32 mm^2/0.8 mm, matrix resolution = 256x256, acquired

resolution = 125x125 μm^2, number of slices = 10, RARE factor = 4 and total scan time = 15 mins. 3D T1WI was acquired using the MPRAGE sequence covering the entire visual pathway, with TI/TR/TE = 2500/9/3ms, FOV = 32x32x11mm, acquisition resolution = 200x200x240μm^3, 1 segment, number of averages = 8 and total scan time = 15 mins.

C. Data Analysis

T1W signal intensities (SI) in the superior colliculi (SC), lateral geniculate nuclei (LGN), primary visual cortex (V1), and V1/V2 transition zone of each hemisphere, and in the splenium of corpus callosum (CC) were measured using ImageJ v1.43u, and were normalized to the surrounding muscles. Mn^{2+} enhancement was quantified by calculating the ratio between left and right visual components in Groups 1 and 2, and the rate of signal increase at Hour 8 and Day 1 compared to Hour 1 in Group 3. Values at each time point were compared to the first time point using two-tailed paired t-tests. Results were considered significant when $p<0.05$.

III. Results

A. Intravitreal, fractionated MEMRI of Retinal and Transsynaptic Connections

In normal adult brains, fractionated, intravitreal Mn^{2+} injection resulted in significant Mn enhancements in contralateral SC and LGN by 45-60% at 1-3 days after initial Mn^{2+} injection, and in contralateral V1 (arrows) by about 10% at 2-3 days after initial Mn^{2+} injection (Fig. 1). Contralateral SC appeared to enhance slightly more than contralateral LGN at all times after initial Mn^{2+} injection.

B. Subcortical, single-dose MEMRI of Thalamo-cortical Connections

Direct, single-dose Mn^{2+} injection to LGN resulted in Mn enhancement by 13-21% in ipsilateral V1 (arrows), and 8-11% in ipsilateral SC at 8-24 hours after Mn^{2+} injection (Fig. 2).

C. Intracortical, single-dose MEMRI of Callosal, Cortico-subcortical and Horizontal Connections

Intracortical, single-dose Mn^{2+} injection to the visual cortex resulted in Mn enhancement by 17-25% in contralateral V1/V2 transition zone (closed arrows), 32-34% in CC (open arrows), 53-65% in ipsilateral dorsal LGN (dashed arrows) and 15-26% in ipsilateral SC at Hours 8-24 (Fig. 2). Notably, some patchy patterns were apparent near the V1/V2 border of the contralateral left hemisphere (Fig. 3), which might be indicative of the ocular dominance domains recently suggested in rodents [48]. Some horizontal cortical connections were also observed in the superficial and middle layers of the ipsilateral hemisphere (Fig. 3)

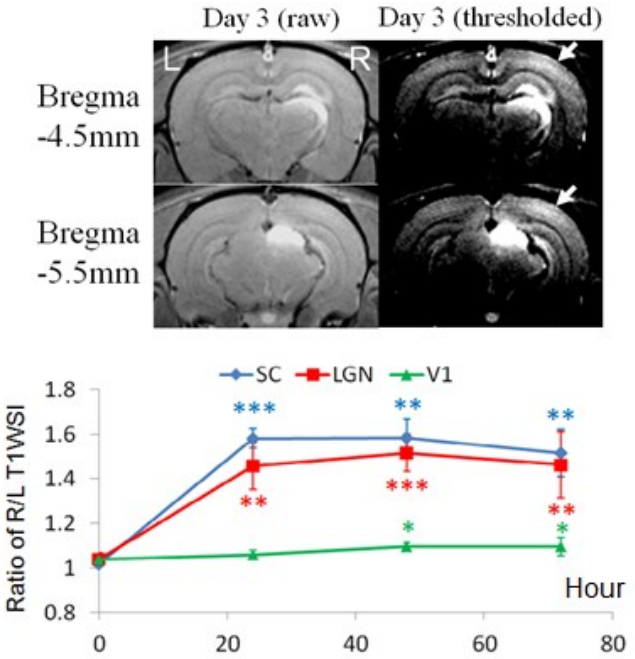

Fig. 1: Intravitreal, fractionated Mn^{2+} injection. (Top) MEMRI at 3 days after initial Mn^{2+} administration to the left eye. (Bottom) Quantitative analyses of T1W SI between right and left SC, LGN and V1 before, and at 1, 2 and 3 days after initial Mn^{2+} injection (Two-tailed paired t-tests with 1st time point, *p<0.05; **p<0.01; ***p<0.001)

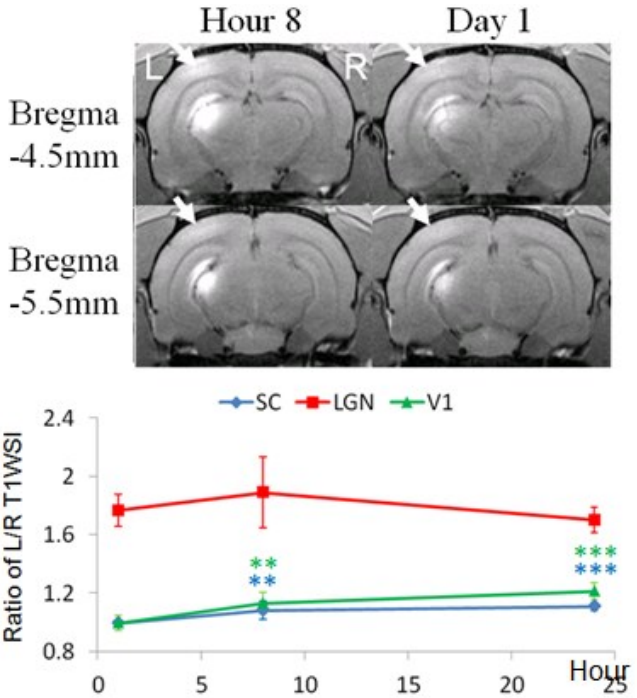

Fig. 2: Subcortical, single-dose Mn^{2+} injection. (Top) MEMRI at 8 hours and 1 day after Mn^{2+} administration to the left LGN. (Bottom) Quantitative analyses of T1W SI between left and right SC, LGN and V1 at 1, 8 and 24 hours after Mn^{2+} injection. (Two-tailed paired t-tests with 1st time point, *p<0.05; **p<0.01; ***p<0.001)

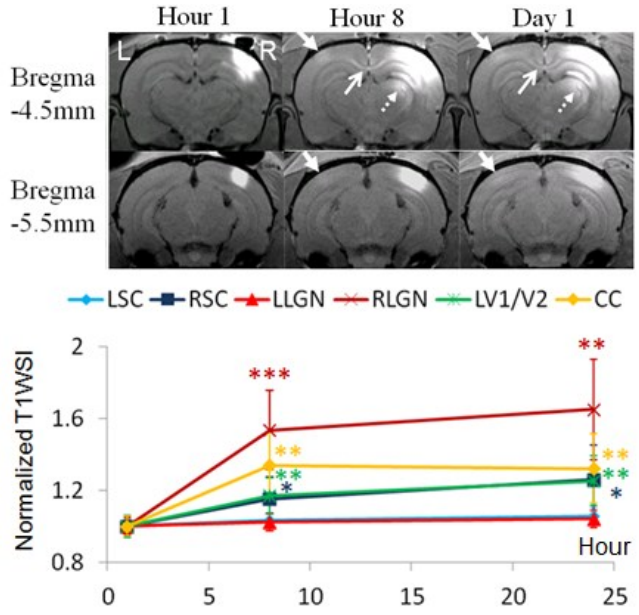

Fig. 3: Intracortical, single-dose Mn^{2+} injection. (Top) MEMRI at 1, 8 and 24 hours after Mn^{2+} administration to the right V1/V2 transition zone. (Bottom) Quantitative analyses of T1W SI of visual components normalized to Hour 1. (Two-tailed paired t-tests with Hour 1, *p<0.05; **p<0.01; ***p<0.001)

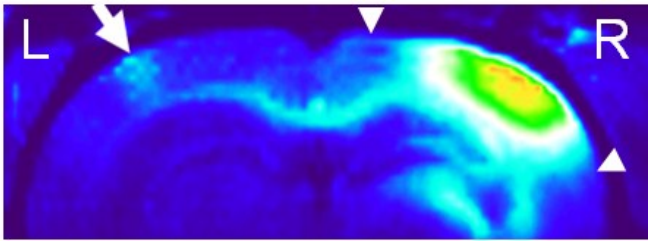

Fig. 4: Reconstructed 3D T1WI of the dorsal brain at 8 hours after right intracortical Mn^{2+} injection. Note the patchy patterns of Mn enhancement in the V1/V2 transition zone of the contralateral left hemisphere (arrow) projected along the visual callosal pathway. The horizontal cortical connections were also observed in the superficial and middle layers of the ipsilateral hemisphere (arrowheads).

IV. Discussions

A. In vivo MEMRI of Retinal, Subcortico-cortical and Transsynaptic Connections

Upon intravitreal Mn^{2+} injection, Mn^{2+} ions were taken up by the RGCs, underwent anterograde axonal transport along retinocollicular and retinogeniculate projections at a rate of 2-6 mm/h, and accumulated at the axonal terminals in the contralateral SC and LGN of the adult rat brain [28, 46]. Although transneuronal transport has been shown to occur in the brain [31], transsynaptic illumination of the visual cortex via intravitreal Mn^{2+} injection has been difficult [49]. Olson et al recently demonstrated that the degree of Mn enhancement in the visual pathway is determined by the duration of availability of Mn^{2+} from the vitreous body but not the injected dose [50]. Given the rapid clearance of Mn from the vitreous body [50], this study evaluated the Mn enhancement in V1 upon (i) fractionated intravitreal injections or (ii) direct, single-dose injection to the LGN. As shown in Figs. 1 and 2, daily, fractionated intravitreal injection resulted in about 10% of Mn enhancement in contralateral V1 starting at Day 2, whereas direct, single-dose injection into the LGN resulted in more than 10% of enhancement in the ipsilateral V1 as early as at 8 hours after injection. The results of these experiments demonstrated the feasibility of MEMRI to evaluate both monosynaptic and polysynaptic anterograde transport in the retinal projections longitudinally upon prolonged Mn input to localized visual components.

B. In vivo MEMRI of Cortico-cortical and Cortico-subcortical Connections

Upon intracortical Mn^{2+} injection, the ipsilateral LGN appeared to enhance at the highest rate than other measured visual components at Hour 8, possibility because of the short distance and high density of cortico-geniculate connections in the visual brain [19]. While the Mn accumulation appeared to slow down from Hours 8 to 24 in the ipsilateral LGN and the CC, the contralateral V1/V2 and ipsilateral SC, whose connections to ipsilateral V1/V2 were more distant, continued to enhance steadily at Hour 24. Recent anatomical and functional studies suggested the presence of ocular dominance domains in the rodent visual cortex [48, 51]. In particular, both histological tracing and electrophysiological experiments demonstrated patches of ipsilateral retinal input in close correlation with callosal patches in the binocular zone of the rat V1 [48]. Our MEMRI observation of the patchy patterns in the callosal projection might provide a new model system for imaging how the precise neuronal connections are shaped by experience in order to study the cellular and molecular mechanisms of ocular dominance plasticity in the critical period [48, 52, 53]. The laminar-specific enhancement in the ipsilateral cortex in Fig. 4 suggested that Mn transport occurred along horizontal connections faster than the diffusion of Mn from the injection site.

V. Conclusions

The results of this study demonstrated the sensitivity of MEMRI for assessing the neuroarchitecture of the visual brains in vivo via 3 different routes of Mn administration without depth-limitation, and may possess great potentials for studying the basic neural components and connections in the visual system longitudinally during development, plasticity, pharmacological interventions and genetic modifications in future studies.

REFERENCES

[1] K. C. Chan, *et al.*, "In vivo multiparametric magnetic resonance imaging and spectroscopy of rodent visual system," *J Integr Neurosci,* vol. 9, pp. 477-508, Dec 2010.

[2] J. Zhang, *et al.*, "Visual map development depends on the temporal pattern of binocular activity in mice," *Nat Neurosci,* vol. 15, pp. 298-307, Feb 2012.

[3] D. S. Greenberg, *et al.*, "Population imaging of ongoing neuronal activity in the visual cortex of awake rats," *Nat Neurosci,* vol. 11, pp. 749-51, Jul 2008.

[4] J. H. Marshel, *et al.*, "Functional specialization of seven mouse visual cortical areas," *Neuron,* vol. 72, pp. 1040-54, Dec 22 2011.

[5] D. Zoccolan, *et al.*, "A rodent model for the study of invariant visual object recognition," *Proc Natl Acad Sci U S A,* vol. 106, pp. 8748-53, May 26 2009.

[6] Q. Wang, *et al.*, "Gateways of ventral and dorsal streams in mouse visual cortex," *J Neurosci,* vol. 31, pp. 1905-18, Feb 2 2011.

[7] K. C. Chan, *et al.*, "Functional MRI of postnatal visual development in normal and hypoxic-ischemic-injured superior colliculi," *Neuroimage,* vol. 49, pp. 2013-20, Feb 1 2010.

[8] C. Lau, *et al.*, "BOLD responses in the superior colliculus and lateral geniculate nucleus of the rat viewing an apparent motion stimulus," *Neuroimage,* vol. 58, pp. 878-84, Oct 1 2011.

[9] C. Lau, *et al.*, "BOLD temporal dynamics of rat superior colliculus and lateral geniculate nucleus following short duration visual stimulation," *PLoS One,* vol. 6, p. e18914, 2011.

[10] K. C. Chan, *et al.*, "GD-DTPA enhanced MRI of ocular transport in a rat model of chronic glaucoma," *Exp Eye Res,* vol. 87, pp. 334-41, Oct 2008.

[11] K. C. Chan, *et al.*, "Late measures of microstructural alterations in severe neonatal hypoxic-ischemic encephalopathy by MR diffusion tensor imaging," *Int J Dev Neurosci,* vol. 27, pp. 607-15, Oct 2009.

[12] K. C. Chan, *et al.*, "Proton magnetic resonance spectroscopy revealed choline reduction in the visual cortex in an experimental model of chronic glaucoma," *Exp Eye Res,* vol. 88, pp. 65-70, Jan 2009.

[13] I. Y. Zhou, *et al.*, "Balanced steady-state free precession fMRI with intravascular susceptibility contrast agent," *Magn Reson Med,* Nov 29 2011.

[14] Y. Kondo, *et al.*, "Bilateral projections of single retinal ganglion cells to the lateral geniculate nuclei and superior colliculi in the albino rat," *Brain Res,* vol. 608, pp. 204-15, Apr 16 1993.

[15] M. Liu, *et al.*, "Dendritic changes in visual pathways in glaucoma and other neurodegenerative conditions," *Exp Eye Res,* vol. 92, pp. 244-50, Apr 2011.

[16] R. D. Lund and J. S. Lund, "Synaptic adjustment after deafferentation of the superior colliculus of the rat," *Science,* vol. 171, pp. 804-7, Feb 26 1971.

[17] A. R. Harvey and D. R. Worthington, "The projection from different visual cortical areas to the rat superior colliculus," *J Comp Neurol,* vol. 298, pp. 281-92, Aug 15 1990.

[18] B. Dreher, *et al.*, "The morphology, number, distribution and central projections of Class I retinal ganglion cells in albino and hooded rats," *Brain Behav Evol,* vol. 26, pp. 10-48, 1985.

[19] K. J. Sanderson, *et al.*, "Prosencephalic connections of striate and extrastriate areas of rat visual cortex," *Exp Brain Res,* vol. 85, pp. 324-34, 1991.

[20] V. M. Montero, "Retinotopy of cortical connections between the striate cortex and extrastriate visual areas in the rat," *Exp Brain Res,* vol. 94, pp. 1-15, 1993.

[21] J. E. Coleman, *et al.*, "Anatomical origins of ocular dominance in mouse primary visual cortex," *Neuroscience,* vol. 161, pp. 561-71, Jun 30 2009.

[22] J. F. Olavarria, *et al.*, "Topography and axon arbor architecture in the visual callosal pathway: effects of deafferentation and blockade of N-methyl-D-aspartate receptors," *Biol Res,* vol. 41, pp. 413-24, 2008.

[23] C. G. Cusick and R. D. Lund, "The distribution of the callosal projection to the occipital visual cortex in rats and mice," *Brain Res,* vol. 214, pp. 239-59, Jun 15 1981.

[24] T. D. Mrsic-Flogel, *et al.*, "Homeostatic regulation of eye-specific responses in visual cortex during ocular dominance plasticity," *Neuron,* vol. 54, pp. 961-72, Jun 21 2007.

[25] S. B. Hofer, *et al.*, "Lifelong learning: ocular dominance plasticity in mouse visual cortex," *Curr Opin Neurobiol,* vol. 16, pp. 451-9, Aug 2006.

[26] Q. Wang, *et al.*, "In vivo transcranial imaging of connections in mouse visual cortex," *J Neurosci Methods,* vol. 159, pp. 268-76, Jan 30 2007.

[27] A. Antonini, *et al.*, "Anatomical correlates of functional plasticity in mouse visual cortex," *J Neurosci,* vol. 19, pp. 4388-406, Jun 1 1999.

[28] R. G. Pautler, *et al.*, "In vivo neuronal tract tracing using manganese-enhanced magnetic resonance imaging," *Magn Reson Med,* vol. 40, pp. 740-8, Nov 1998.

[29] G. Soria, *et al.*, "Reproducible imaging of rat corticothalamic pathway by longitudinal manganese-enhanced MRI (L-MEMRI)," *Neuroimage,* vol. 41, pp. 668-74, Jul 1 2008.

[30] J. Tucciarone, *et al.*, "Layer specific tracing of corticocortical and thalamocortical connectivity in the rodent using manganese enhanced MRI," *Neuroimage,* vol. 44, pp. 923-31, Feb 1 2009.

[31] R. G. Pautler, "In vivo, trans-synaptic tract-tracing utilizing manganese-enhanced magnetic resonance imaging (MEMRI)," *NMR Biomed,* vol. 17, pp. 595-601, Dec 2004.

[32] S. Canals, *et al.*, "Magnetic resonance imaging of cortical connectivity in vivo," *Neuroimage,* vol. 40, pp. 458-72, Apr 1 2008.

[33] K. C. Chan, *et al.*, "In vivo retinotopic mapping of superior colliculus using manganese-enhanced magnetic resonance imaging," *Neuroimage,* vol. 54, pp. 389-395 2011/01/01 2011.

[34] K. C. Chan, *et al.*, "In vivo evaluation of retinal and callosal projections in early postnatal development and plasticity using manganese-enhanced MRI and diffusion tensor imaging," *Neuroimage,* Oct 1 2011.

[35] K. C. Chan, *et al.*, "Evaluation of the retina and optic nerve in a rat model of chronic glaucoma using in vivo manganese-enhanced magnetic resonance imaging," *Neuroimage,* vol. 40, pp. 1166-74, Apr 15 2008.

[36] K. C. Chan, *et al.*, "In vivo chromium-enhanced MRI of the retina," *Magn Reson Med,* Dec 28 2011.

[37] Y. X. Liang, *et al.*, "CNS regeneration after chronic injury using a self-assembled nanomaterial and MEMRI for real-time in vivo monitoring," *Nanomedicine,* vol. 7, pp. 351-9, Jun 2011.

[38] K. C. Chan, *et al.*, "Evaluation of the visual system in a rat model of chronic glaucoma using manganese-enhanced magnetic resonance imaging," *Conf Proc IEEE Eng Med Biol Soc,* vol. 2007, pp. 67-70, 2007.

[39] I. Aoki, *et al.*, "In vivo detection of neuroarchitecture in the rodent brain using manganese-enhanced MRI," *Neuroimage,* vol. 22, pp. 1046-59, Jul 2004.

[40] A. C. Silva, *et al.*, "Detection of cortical laminar architecture using manganese-enhanced MRI," *J Neurosci Methods,* vol. 167, pp. 246-57, Jan 30 2008.

[41] J. Yang, *et al.*, "Manganese-enhanced MRI detection of neurodegeneration in neonatal hypoxic-ischemic cerebral injury," *Magn Reson Med,* vol. 59, pp. 1329-39, Jun 2008.

[42] J. Yang and E. X. Wu, "Detection of cortical gray matter lesion in the late phase of mild hypoxic-ischemic injury by manganese-enhanced MRI," *Neuroimage,* vol. 39, pp. 669-79, Jan 15 2008.

[43] K. C. Chan, *et al.*, "Early detection of neurodegeneration in brain ischemia by manganese-enhanced MRI," *Conf Proc IEEE Eng Med Biol Soc,* vol. 2008, pp. 3884-7, 2008.

[44] X. Yu, *et al.*, "In vivo auditory brain mapping in mice with Mn-enhanced MRI," *Nat Neurosci,* vol. 8, pp. 961-8, Jul 2005.

[45] D. Bissig and B. A. Berkowitz, "Same-session functional assessment of rat retina and brain with manganese-enhanced MRI," *Neuroimage,* vol. 58, pp. 749-60, Oct 1 2011.

[46] T. Watanabe, *et al.*, "Functional mapping of neural pathways in rodent brain in vivo using manganese-enhanced three-dimensional magnetic resonance imaging," *NMR Biomed,* vol. 17, pp. 554-68, Dec 2004.

[47] Y. J. Lin and A. P. Koretsky, "Manganese ion enhances T1-weighted MRI during brain activation: an approach to direct imaging of brain function," *Magn Reson Med,* vol. 38, pp. 378-88, Sep 1997.

[48] R. Liang, *et al.*, "Segregated ocular dominance domains in rat visual cortex: Anatomical and physiological evidence," presented at the Abstr Soc for Neurosci, 2010.

[49] J. D. Lindsey, *et al.*, "Magnetic resonance imaging of the visual system in vivo: transsynaptic illumination of V1 and V2 visual cortex," *Neuroimage,* vol. 34, pp. 1619-26, Feb 15 2007.

[50] O. Olsen, *et al.*, "Manganese transport in the rat optic nerve evaluated with spatial- and time-resolved magnetic resonance imaging," *J Magn Reson Imaging,* vol. 32, pp. 551-60, Sep 2010.

[51] C. Cerri, *et al.*, "Callosal contribution to ocular dominance in rat primary visual cortex," *Eur J Neurosci,* vol. 32, pp. 1163-9, Oct 2010.

[52] C. L. McCurry, *et al.*, "Loss of Arc renders the visual cortex impervious to the effects of sensory experience or deprivation," *Nat Neurosci,* vol. 13, pp. 450-7, Apr 2010.

[53] A. Maffei, *et al.*, "Critical period for inhibitory plasticity in rodent binocular V1," *J Neurosci,* vol. 30, pp. 3304-9, Mar 3 2010.